PLANT SPECIFIC FAST NEUTRON EXPOSURE EVALUATIONS FOR THE FIRST 20 OPERATING FUEL CYCLES OF THE YANKEE ROWE REACTOR

Stanwood L. Anderson

November 1990

Work performed under Shop Order No. YAOP-450G

WESTINGHOUSE ELECTRIC CORPORATION
Energy Systems Business Unit
P. O. Box 355
Pittsburgh, Pennsylvania 15230

1.0 BASELINE NEUTRON TRANSPORT CALCULATIONS

The fast neutron fluence evaluations for the Yankee Rowe reactor were carried out using both one- and two-dimensional discrete ordinates techniques. Two-dimensional computations were completed with the DOT code [1] run in both the forward and adjoint mode. The ANISN discrete ordinates code [2] was utilized to perform the required one-dimensional analyses. All of the two-dimensional cases were run in R,Theta geometry, while, the corresponding one-dimensional runs were carried out using the cylindrical geometry option.

1.1 Geometric Modeling

The geometric models used in the fluence evaluations were based on design drawings of the plant with adjustments to the design based on available as-built measurements. In particular, as-built information was employed to establish the inner radius and thickness of the pressure vessel as well as the location and thickness of the thermal shield.

A plan view of the Yankee Rowe reactor geometry at the core midplane elevation is shown in Figure 1-1. This model was based on information from the following Westinghouse reactor design drawings: 646J500, 646J614, 549D155, 540F839, 540F857, 646J692, 673C510, and 673C511; on Babcock and Wilcox drawings 45109E, 71695E0 and 66042E; and on Stone & Webster drawings 9699-FV-2A and 9699-FV-2B. Also utilized in the development of this model was additional as-built dimensional information provided by Yankee Atomic Electric Company.

The analysis of the 1/8 core sector shown as 0-45 degrees on Figure 1-1 was used as the baseline for the transport evaluations. In terms of the baffle support structure and thermal shield brackets, the chosen sector minimizes the amount of steel between the reactor core and the pressure vessel resulting in conservative evaluation of the vessel exposure.

The mesh line schematic used in the R,Theta analysis for the 0-45 sector shown in Figure 1-1 is depicted in Figure 1-2. The radial and azimuthal mesh line dimensions corresponding to Figure 1-2 are given in Tables 1-1 and 1-2, respectively.

In addition to the two-dimensional calculations, several one-dimensional computations were also carried out to establish adjustment factors for the final results and to perform sensitivity studies of several of the input variables. In establishing a geometric model for the one-dimensional calculations, the radial mesh from the first theta interval shown in Figure 1-1 were taken as a representative configuration. However, since, in the theta sense, they are not global to the overall problem the baffle support structure and thermal shield strap were removed from the geometry. The radial mesh line schematic for the one-dimensional model is shown in Figure 1-3. The mesh line dimensions for this model were taken from Table 1-1.

FIGURE 1-1

PLAN VIEW OF THE YANKEE ROWE REACTOR GEOMETRY AT CORE MIDPLANE
0 - 90 DEGREE SECTOR

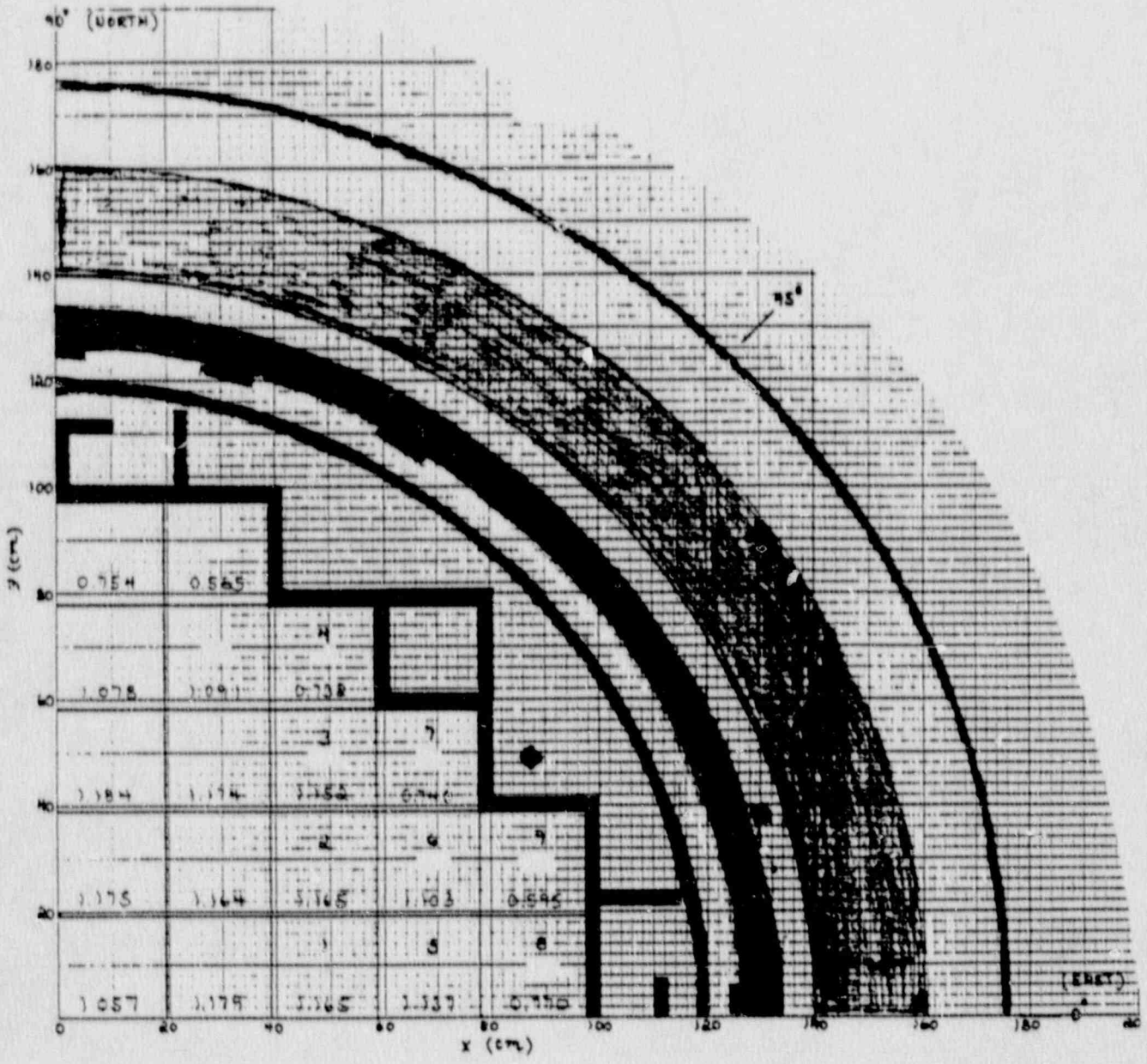

FIGURE 1-2

MESH LINE SCHEMATIC USED IN THE R,THETA ANALYSIS
OF THE YANKEE ROWE REACTOR
θ - 45 DEGREE SECTOR

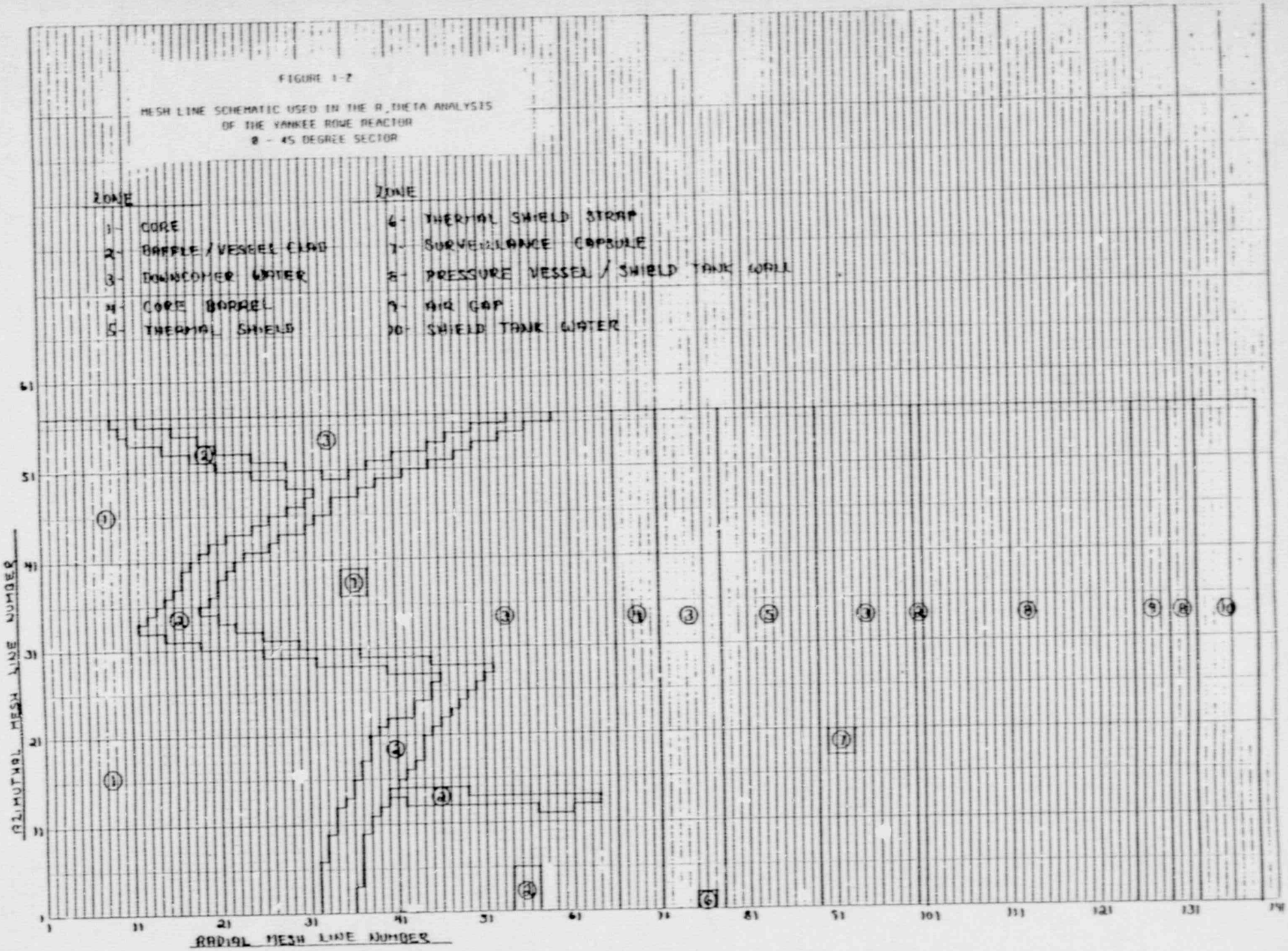

TABLE 1-1

RADIAL MESH LINE DIMENSIONS FOR THE R,THETA MODEL
OF THE YANKEE ROWE REACTOR
0 - 45 DEGREE SECTOR

LINE No	RADIUS (cm)	LINE No	RADIUS (cm)	LINE No	RADIUS (cm)	LINE No	RADIUS (cm)
1	55.14	36	99.78	71	120.33	106	143.54
2	60.00	37	100.52	72	121.25	107	144.43
3	65.00	38	101.26	73	122.18	108	145.31
4	70.00	39	101.45	74	123.10	109	146.19
5	75.00	40	101.93	75	124.02	110	147.07
6	80.00	41	102.44	76	124.97	111	147.95
7	82.00	42	102.86	77	125.92	112	148.83
8	83.00	43	103.09	78	126.51	113	149.71
9	83.44	44	103.79	79	127.26	114	150.59
10	84.96	45	104.34	80	128.01	115	151.48
11	86.57	46	104.98	81	128.76	116	152.36
12	87.08	47	105.46	82	129.51	117	153.24
13	87.44	48	106.10	83	130.26	118	154.12
14	87.91	49	106.78	84	131.01	119	155.00
15	88.31	50	107.35	85	131.76	120	155.88
16	88.73	51	107.72	86	132.51	121	156.76
17	89.59	52	108.25	87	133.26	122	157.65
18	90.05	53	108.89	88	134.01	123	158.53
19	90.50	54	109.20	89	134.76	124	159.41
20	91.46	55	110.17	90	134.78	125	160.29
21	91.95	56	110.80	91	135.52	126	164.03
22	92.46	57	111.74	92	136.26	127	167.78
23	92.75	58	112.08	93	137.00	128	171.52
24	93.45	59	112.93	94	137.38	129	175.26
25	93.73	60	113.77	95	137.77	130	175.90
26	94.02	61	114.62	96	138.15	131	176.53
27	94.62	62	115.25	97	138.54	132	177.17
28	95.47	63	115.89	98	138.92	133	178.00
29	95.87	64	116.52	99	139.31	134	180.00
30	96.47	65	117.16	100	139.69	135	183.00
31	96.82	66	117.79	101	139.97	136	187.00
32	97.63	67	118.30	102	140.30	137	191.00
33	98.10	68	118.81	103	140.90	138	195.00
34	98.73	69	119.32	104	141.78	139	200.00
35	99.04	70	119.82	105	142.66		

TABLE 1-2

AZIMUTHAL MESH LINE DIMENSIONS FOR THE R,THETA MODEL
OF THE YANKEE ROWE REACTOR
0 - 45 DEGREE SECTOR

LINE No	THETA (deg)	THETA (rev)	LINE No	THETA (deg)	THETA (rev)
1	0.00	0.00000	29	23.00	0.06389
2	1.00	0.00278	30	24.00	0.06667
3	2.00	0.00556	31	25.00	0.06944
4	3.00	0.00833	32	26.00	0.07222
5	3.85	0.01069	33	26.40	0.07333
6	4.00	0.01111	34	26.80	0.07444
7	5.00	0.01389	35	27.00	0.07500
8	6.00	0.01667	36	28.00	0.07778
9	7.00	0.01944	37	28.41	0.07893
10	8.00	0.02222	38	28.83	0.08008
11	9.00	0.02500	39	29.26	0.08128
12	9.28	0.02578	40	29.68	0.08246
13	10.00	0.02778	41	30.00	0.08333
14	11.00	0.03056	42	31.00	0.08611
15	12.00	0.03333	43	32.00	0.08889
16	13.00	0.03611	44	33.00	0.09167
17	14.00	0.03889	45	34.00	0.09444
18	15.00	0.04167	46	35.00	0.09722
19	16.03	0.04453	47	36.00	0.1000
20	16.34	0.04539	48	36.70	0.1019
21	16.66	0.04628	49	37.10	0.1031
22	16.97	0.04714	50	38.00	0.1056
23	18.00	0.05000	51	39.00	0.1083
24	19.00	0.05278	52	40.00	0.1111
25	20.00	0.05556	53	41.00	0.1139
26	21.00	0.05833	54	42.00	0.1167
27	21.60	0.06000	55	43.00	0.1194
28	22.00	0.06111	56	44.00	0.1222
			57	45.00	0.1250

FIGURE 1-3

MESH LINE SCHEMATIC FOR THE ONE-DIMENSIONAL
MODEL OF THE YANKEE ROWE REACTOR

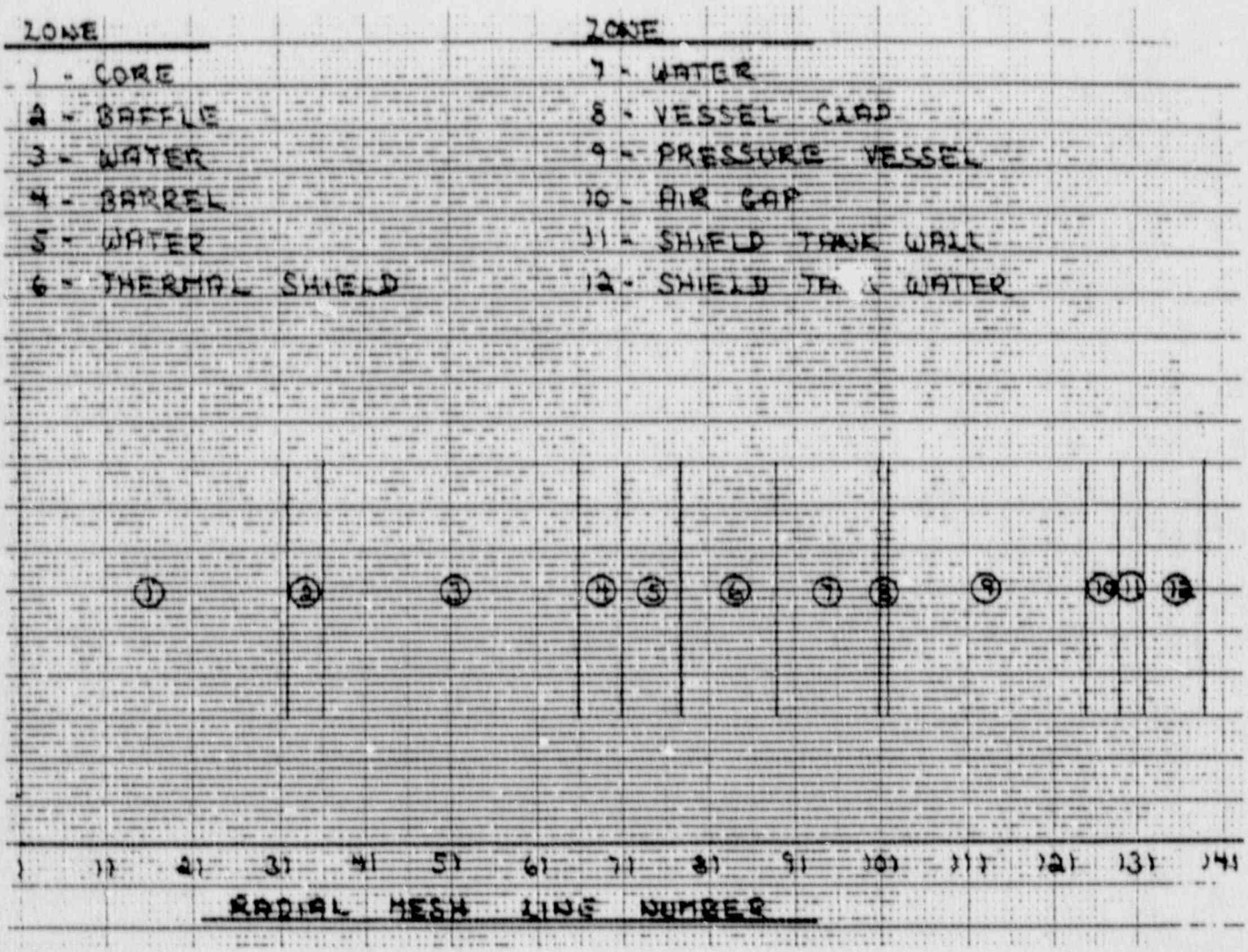

1.2 Material Descriptions

Core Region

Over the 20 operating cycles of the Yankee-Rowe reactor, fuel of varying designs has been supplied by several vendors. Examples of the core compositions for each of these fuel types were supplied by Yankee Atomic Electric Company [3].

For the purposes of this study, two of these core compositions were pursued further. An all zirconium clad core supplied by Combustion Engineering for fuel cycles 18-20 was used in all of the two-dimensional calculations, both forward and adjoint; while a stainless steel clad, Westinghouse designed core composition employed during cycles 1-11 was used in one-dimensional analyses designed to determine the degree of fluence reduction afforded by the lower leakage core used during the earlier plant operation. Fuel designs utilized in cycles 12-17 were similar to the zirconium core design implemented in cycles 18-20 and were not explicitly factored into the analyses.

The resultant number densities computed for the two homogeneous core zones used in the one and two dimensional discrete ordinates calculations were as follows:

Number Density (atom/barn-cm)

	Zirconium Core	Stainless Steel Core
U-235	2.705E-04	3.824E-04
U-238	6.666E-03	7.359E-03
O (fuel)	1.387E-02	1.548E-02
O (water)	1.336E-02	1.231E-02
H	2.671E-02	2.461E-02
Zr	7.317E-03	2.688E-03
Fe		6.769E-03
Mn		2.007E-04
Cr		2.014E-03
Ni		8.730E-04
Si		1.962E-04
C		3.670E-05

Stainless Steel/Carbon Steel

For the reactor internals, pressure vessel, and shield tank wall, nominal stainless steel and carbon steel compositions were employed. The number densities used to generate macroscopic cross-sections for these materials were as follows:

	Number Density (atom/barn-cm)	
	Stainless Steel	Carbon Steel
Fe	5.943E-02	8.270E-02
Mn	1.762E-03	1.116E-03
Cr	1.768E-02	
Ni	7.665E-03	4.420E-04
Si	1.723E-03	
C	3.222E-04	9.819E-04

Water

In the various transport calculations, water cross-sections were required for the following conditions.

Temperature (deg F)	Pressure (psi)	Density (g/cm3)
535	2000	0.7629
525	2000	0.7725
500	2000	0.7951
450	2000	0.8345
72	(atm)	1.00

The corresponding number densities computed for these pressure/temperature conditions were as follows:

	Number density (atom/barn-cm)				
	535 F	525 F	500 F	450 F	72 F
H	5.104E-02	5.168E-02	5.320E-02	5.582E-02	6.690E-02
O	2.552E-02	2.584E-02	2.660E-02	2.791E-02	3.345E-02

Macroscopic cross-sections for use in the fluence evaluations were developed from the SAILOR library [4] using the P3, 47 group data. The SAILOR library is an ENDFB-IV data set developed explicitly for light water reactor applications. The data set is available from the ORNL Radiation Shielding Information Center (RSIC) as data set DLC-76.

1.3 Neutron Transport Calculation

FORWARD CALCULATIONS

In performing the plant specific fluence evaluations, several sets of transport calculations were carried out. The first series of calculations consisted of three forward computations with variable water temperature in the downcomer regions. The purpose of these calculations was to provide azimuthally dependent correction factors to account for the impact of reduced temperature operation that occured during coastdown periods at the end of each fuel cycle.

The forward calculations utilized the geometric representation of the 0-45 degree sector of the reactor geometry described in Section 1.1. The calculations were run in R,theta geometry using a P3 cross-section expansion and an S8 order of angular quadrature. The core source utilized in each of the computations was representative of the burnup weighted average of 20 cycles of source data supplied by Yankee Atomic Electric Company [3].

A summary of the core power distribution information used in the calculations is provided in Table 1-3. In regard to Table 1-3, the fuel assembly identification numbers correlate with those specified in Figure 1-1. Also shown on the table are the core coordinates specified in reference 3. The power distribution data itself represents the relative power in each fuel assembly averaged over the individual fuel cycles. The burnup weighted relative assembly powers from Table 1-3 were employed to provide the base case source distribution for use in the forward transport calculations.

In developing the source distribution for the transport calculations, the within assembly spatial gradients were approximated with representative pin by pin power distributions also supplied by Yankee Atomic Electric Company [5]. As noted in reference 5, these pin by pin distributions were taken from the core design analysis for fuel cycle 19. These relative spatial gradients were taken as representative of operation over the entire life of the unit.

In addition to the relative assembly powers and within assembly gradients, Yankee Atomic also supplied axial peaking factors for each fuel cycle [3]. These peaking factors, representing the maximum flux location, are also listed on Table 1-3. The burnup weighted axial peaking factor of 1.22 was used in the computation of the normalization factor for the forward DOT runs along with a nominal core power level of 600 MWt.

Using the flux (E > 1.0 Mev) response from a series of three DOT runs with downcomer temperatures of 450, 500, and 525 degrees F permits the determination of the impact of downcomer water temperature on vessel exposure rates as a function of azimuthal angle. The results of this evaluation are provided in Figure 1-4 and Table 1-4. In this relative comparison, the 500 F case was taken to be the baseline and data for intermediate temperatures were taken from the curves shown in Figure 1-4. The data extracted from the DOT runs to generate the temperature sensitivity study were taken from the vessel cladding at 14.5 and 44.5 degree azimuthal locations. These particular azimuths were taken as representative of the maximum and minimum exposure of the vessel.

TABLE 1-3

SUMMARY OF RELATIVE CORE POWER DISTRIBUTIONS
FOR THE YANKEE ROWE REACTOR

CYCLE No.	AVERAGE BURNUP (MWD/MTU)	FUEL ASSEMBLY ID H6 1	H7 2	H8 3	H9 4	J6 5	J7 6	J8 7	K6 8	K7 9	Fa
1	8470	1.320	1.290	1.070	0.570	1.020	0.930	0.590	0.580	0.440	1.250
2	7866	1.400	1.330	1.040	0.520	1.020	0.970	0.560	0.600	0.420	1.250
3	6329	1.252	1.223	1.096	0.668	1.060	1.014	0.718	0.689	0.542	1.250
4	8734	1.314	1.245	1.097	0.651	1.111	1.023	0.651	0.656	0.504	1.250
5	8893	1.183	1.179	1.213	0.777	1.097	1.145	0.777	0.770	0.615	1.250
6	12419	1.316	1.221	1.115	0.655	1.100	1.041	0.655	0.657	0.501	1.250
7	11963	1.231	1.230	1.105	0.748	1.157	1.114	0.748	0.747	0.585	1.250
8	10142	1.241	1.241	1.148	0.727	1.152	1.086	0.727	0.727	0.574	1.250
9	11946	1.206	1.216	1.200	0.677	1.125	1.149	0.654	0.849	0.503	1.250
10	15148	1.115	1.164	1.219	0.864	1.110	1.127	0.871	0.861	0.666	1.250
11	12869	1.166	1.195	1.222	0.770	1.165	1.192	0.804	0.824	0.653	1.250
12	14879	1.101	1.203	1.173	0.732	1.224	1.144	0.775	0.787	0.620	1.250
13	12890	1.079	1.151	1.190	0.789	1.102	1.133	0.793	0.801	0.640	1.200
14	16114	1.132	1.175	1.143	0.708	1.207	1.100	0.719	0.749	0.583	1.200
15	13000	1.101	1.174	1.156	0.760	1.125	1.099	0.765	0.775	0.618	1.200
16	14168	1.095	1.150	1.149	0.746	1.200	1.116	0.757	0.778	0.624	1.175
17	15116	1.158	1.062	1.158	0.756	1.080	1.129	0.752	0.806	0.628	1.175
18	16020	1.073	1.058	1.138	0.743	1.222	1.109	0.739	0.814	0.626	1.175
19	15518	1.153	1.053	1.159	0.782	1.068	1.130	0.787	0.818	0.654	1.175
20	16850	1.043	1.031	1.140	0.765	1.203	1.113	0.760	0.831	0.650	1.175
AVG.	249334	1.165	1.165	1.152	0.732	1.137	1.103	0.740	0.770	0.595	1.218

The calculated values for flux (E > 1.0 Mev) at the vessel cladding from the 500 F base case are shown graphically as a function of azimuthal angle in Figure 1-5. From Figure 1-5, it is noted that the maximum fast flux occurs in the 12 to 17 degree range relative to the cardinal axes and the minimum occurs at the 45 degree location.

ADJOINT CALCULATIONS

In order to perform the fuel cycle specific evaluations, adjoint transport calculations based on source points in the vessel cladding zone were carried out for azimuthal locations representing the maximum and minimum exposure of the pressure vessel wall. These azimuthal locations were 14.5 degrees for the maximum and 44.5 degrees for the minimum. Both calculations were carried out using the DOT code with P3 scattering cross-sections and an S8 angular quadrature. The geometric model used in these evaluations was the same as that shown in Figure 1-2. The adjoint source term used in both calculations was the fast neutron flux (E > 1.0 MeV).

Following completion of the adjoint DOT computations, the output adjoint fluxes were processed to provide importance function input to be used in evaluating each individual fuel cycle. Using the importance functions developed from the adjoint DOT runs along with the power distributions for each fuel cycle, calculations were then carried out to determine the cycle specific neutron exposure of the reactor vessel.

In performing the cycle specific fluence calculations, each fuel cycle was subdivided into a period of power operation and a coastdown interval resulting in a total of 40 operating periods. The calculations made use of power distributions given in Table 1-3 with the same power distribution assumed to apply for both subdivisions of each cycle. Temperature corrections from Figure 1-4 were used in conjunction with downcomer temperatures from reference 3 in computing the normalization of the fluence results for each period of operation. Cycle specific values of axial peaking factors were taken from Table 1-3; and, again, the individual factors were assumed to apply to both power operation and coastdown periods. A radial translation factor of 0.987, developed from the 500 F forward DOT run was also used to translate results from the cladding mid-mesh to the actual clad/base metal interface.

The impact of the stainless steel clad core was evaluated with two one-dimensional transport calculations using the ANISN code in cylindrical geometry. The one-dimensional geometric model was as shown in Figure 1-3. The calculations were carried out using the same P3 cross-section sets as were used in the DOT calculations and an S8 order of angular quadrature. The problems were normalized to a core source of 1.0 n/cm-sec and utilized the radial spatial distribution of source from the 0 degree azimuth in the DOT calculations. A comparison of the ANISN results at the pressure vessel clad

FIGURE 1-4

EFFECT OF DOWNCOMER WATER TEMPERATURE ON THE FAST NEUTRON FLUX (E > 1.0 MeV) INCIDENT ON THE PRESSURE VESSEL INNER RADIUS

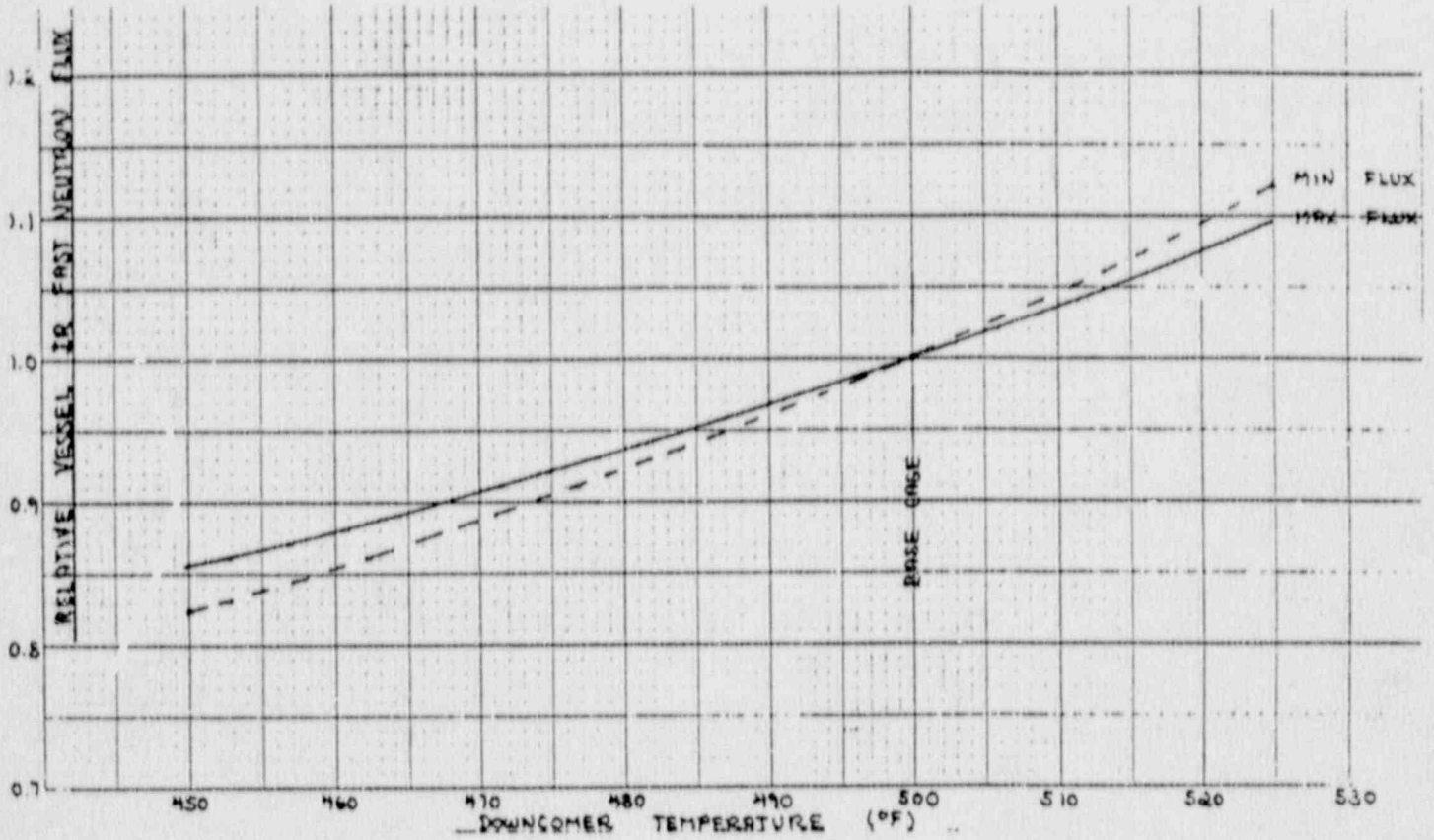

TABLE 1-4

EFFECT OF DOWNCOMER WATER TEMPERATURE ON THE FAST NEUTRON FLUX (E > 1.0 MeV) INCIDENT ON THE PRESSURE VESSEL INNER RADIUS

INLET TEMPERATURE (Deg F)	MAXIMUM FLUX (n/cm2-sec)	MINIMUM FLUX (n/cm2-sec)
450	0.855	0.823
455	0.868	0.839
460	0.880	0.853
465	0.892	0.871
470	0.908	0.888
475	0.921	0.904
480	0.937	0.922
485	0.951	0.941
490	0.969	0.960
495	0.983	0.980
500	1.000	1.000
505	1.018	1.023
510	1.036	1.045
515	1.055	1.070
520	1.074	1.094
525	1.096	1.122

FIGURE 1-5

FAST NEUTRON FLUX (E > 1.0 MeV) AS A FUNCTION OF
AZIMUTHAL ANGLE WITHIN THE PRESSURE VESSEL CLADDING
500 DEGREE F BASE CASE CALCULATION

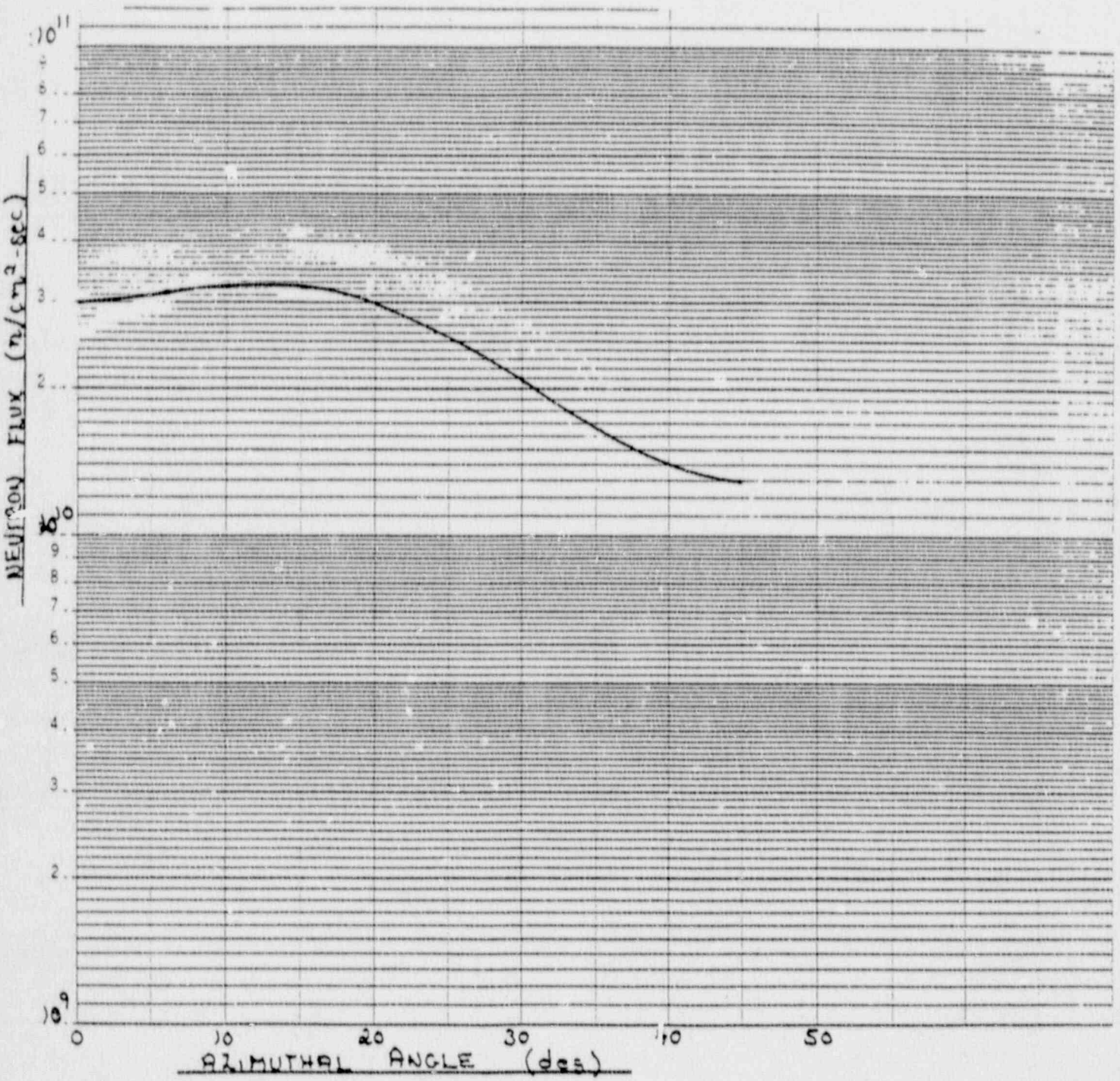

yielded a value of 0.911 for the fuel adjustment factor for cycles 1-9. This adjustment for the presence of stainless steel clad fuel was used for fuel cycles 1 through 9 which represent the cycles that included stainless fuel on the periphery of the core. Although stainless clad fuel was also present during cycles 10 and 11, the assemblies were interior to the core and no credit was taken for their presence.

Cycle lengths and downcomer temperatures were taken directly from reference 3. The individual cycle correction factors to account for axial peaking factors, temperature variations, and fuel composition are summarized in Table 1-5

Results of the individual adjoint calculations are summarized in Tables 1-6 and 1-7 for the 14.5 degree and 44.5 degree locations, respectively. A fast neutron (E > 1.0 Mev) fluence profile was developed for the end of cycle 20 by normalizing the azimuthal flux shape from the 500 F base case transport calculation to the cycle specific calculations at the 14.5 and 44.5 degree locations. Since the forward DOT utilized the 20 cycle average core power distribution as input, the calculated azimuthal shape should be quite representative. The appropriate normalization factors were computed as follows by dividing the cycle specific fluence by the DOT calculated flux in the vessel cladding.

	14.5 DEG	44.5 DEG
CYCLE SPECIFIC FLUENCE	2.13E+19	8.52E+18
DOT FLUX	3.26E+10	1.30E+10
NORMALIZATION	6.53E+08	6.55E+08

The agreement between the normalization factors calculated for the maximum and minimum vessel flux locations lends support to the use of the azimuthal shape taken from the forward DOT calculation. In developing the final fluence profile for the vessel inner radius, the average value of these normalization factors was used; i.e., 6.54E+08. A summary of the calculated azimuthal fluence profile is presented in tabular form in Table 1-8 and illustrated graphically in Figure 1-6.

The fluence values provided in Table 1-8 and Figure 1-6 are representative of the clad/base metal interface at the axial location of the peak flux in the 0-45 degree sector. The actual axial location of the peak cannot be documented here, since Yankee Atomic supplied no axial profiles but, only a single peaking factor for each cycle. Again, the data are applicable to the end of fuel cycle 20 and are representative of 6.77E+08 effective full power seconds (21.45 EFPY) of operation.

In addition to the fluence at the vessel inner radius, the distribution of fluence through the thickness of the pressure vessel wall is of interest. Tabulations of the fluence distribution at the maximum and minimum exposure locations are given in Table 1-9. The radial distributions were obtained by normalizing the radial flux profiles from the 500 F forward DOT to the relative distributions given in Table 1-9.

TABLE 1-5

SUMMARY OF CYCLE DEPENDENT ADJUSTMENT FACTORS
USED TO DERIVE CYCLE SPECIFIC FAST NEUTRON FLUENCE

CYCLE	AXIAL PEAKING FACTOR	FUEL FACTOR	COOLANT TEMP DEG F	TEMPERATURE FACTOR 14.5 DEG	TEMPERATURE FACTOR 44.5 DEG
1P	1.250	0.911	500	1.000	1.000
1C	1.250	0.911	454	0.863	0.836
2P	1.250	0.911	496	0.988	0.983
2C	1.250	0.911	464	0.890	0.867
3P	1.250	0.911	501	1.001	1.003
3C	1.250	0.911	473	0.916	0.898
4P	1.250	0.911	507	1.025	1.032
4C	1.250	0.911	478	0.931	0.915
5P	1.250	0.911	505	1.018	1.022
5C	1.250	0.911	489	0.965	0.957
6P	1.250	0.911	505	1.018	1.022
6C	1.250	0.911	484	0.949	0.938
7P	1.250	0.911	505	1.018	1.022
7C	1.250	0.911	482	0.942	0.930
8P	1.250	0.911	507	1.025	1.032
8C	1.250	0.911	491	0.971	0.963
9P	1.250	0.911	507	1.025	1.032
9C	1.250	0.911	488	0.964	0.952
10P	1.250	1.000	503	1.011	1.013
10C	1.250	1.000	479	0.933	0.920
11P	1.250	1.000	509	1.032	1.041
11C	1.250	1.000	493	0.978	0.972
12P	1.250	1.000	504	1.014	1.020
12C	1.250	1.000	492	0.973	0.968
13P	1.200	1.000	503	1.011	1.013
13C	1.200	1.000	499	0.996	0.995
14P	1.200	1.000	512	1.043	1.053
14C	1.200	1.000	482	0.942	0.930
15P	1.200	1.000	510	1.036	1.045
15C	1.200	1.000	493	0.978	0.972
16P	1.175	1.000	511	1.040	1.050
16C	1.175	1.000	504	1.014	1.019
17P	1.175	1.000	513	1.048	1.060
17C	1.175	1.000	487	0.959	0.950
18P	1.175	1.000	511	1.040	1.050
18C	1.175	1.000	493	0.978	0.972
19P	1.175	1.000	509	1.032	1.041
19C	1.175	1.000	482	0.942	0.930
20P	1.175	1.000	512	1.043	1.053
20C	1.175	1.000	491	0.971	0.963

TABLE 1-6

SUMMARY OF CYCLE SPECIFIC FAST NEUTRON FLUX AND FLUENCE
AT THE 14.5 DEGREE VESSEL INNER RADIUS LOCATION

CYCLE NO.	CYCLE TIME (efps)	CUMULATIVE TIME (efps)	CYCLE AVERAGE FLUX (n/cm2-sec)	CUMULATIVE FLUENCE (n/cm2)
1P	1.87E+07	1.87E+07	2.32E+10	4.33E+17
1C	6.45E+06	2.52E+07	2.00E+10	5.62E+17
2P	1.76E+07	4.28E+07	2.28E+10	9.63E+17
2C	6.04E+06	4.88E+07	2.04E+10	1.09E+18
3P	9.90E+06	5.87E+07	2.74E+10	1.36E+18
3C	9.15E+06	6.78E+07	2.51E+10	1.59E+18
4P	1.70E+07	8.48E+07	2.68E+10	2.04E+18
4C	9.03E+06	9.39E+07	2.42E+10	2.26E+18
5P	2.19E+07	1.16E+08	3.13E+10	2.95E+18
5C	4.90E+06	1.21E+08	2.96E+10	3.09E+18
6P	2.82E+07	1.49E+08	2.66E+10	3.84E+18
6C	9.26E+06	1.58E+08	2.46E+10	4.07E+18
7P	2.70E+07	1.85E+08	3.02E+10	4.88E+18
7C	8.78E+06	1.94E+08	2.80E+10	5.13E+18
8P	2.43E+07	2.18E+08	2.98E+10	5.85E+18
8C	5.59E+06	2.24E+08	2.82E+10	6.01E+18
9P	2.97E+07	2.54E+08	2.96E+10	6.89E+18
9C	6.24E+06	2.60E+08	2.78E+10	7.07E+18
10P	2.94E+07	2.89E+08	3.69E+10	8.15E+18
10C	1.05E+07	3.00E+08	3.41E+10	8.51E+18
11P	2.92E+07	3.29E+08	3.70E+10	9.59E+18
11C	4.67E+06	3.34E+08	3.49E+10	9.75E+18
12P	3.68E+07	3.70E+08	3.49E+10	1.10E+19
12C	1.83E+06	3.72E+08	3.35E+10	1.11E+19
13P	3.20E+07	4.04E+08	3.37E+10	1.22E+19
13C	1.01E+06	4.05E+08	3.34E+10	1.22E+19
14P	3.57E+07	4.41E+08	3.26E+10	1.34E+19
14C	5.66E+06	4.47E+08	2.93E+10	1.35E+19
15P	3.00E+07	4.77E+08	3.35E+10	1.45E+19
15C	3.92E+06	4.80E+08	3.19E+10	1.47E+19
16P	3.51E+07	5.16E+08	3.33E+10	1.58E+19
16C	1.43E+06	5.17E+08	3.25E+10	1.59E+19
17P	3.30E+07	5.50E+08	3.39E+10	1.70E+19
17C	5.47E+06	5.55E+08	3.10E+10	1.72E+19
18P	3.63E+07	5.92E+08	3.38E+10	1.84E+19
18C	4.37E+06	5.96E+08	3.18E+10	1.85E+19
19P	3.24E+07	6.29E+08	3.42E+10	1.97E+19
19C	6.36E+06	6.35E+08	3.13E+10	1.99E+19
20P	3.76E+07	6.72E+08	3.50E+10	2.12E+19
20C	4.44E+06	6.77E+08	3.23E+10	2.13E+19

TABLE 1-7

SUMMARY OF CYCLE SPECIFIC FAST NEUTRON FLUX AND FLUENCE
AT THE 44.5 DEGREE VESSEL INNER RADIUS LOCATION

CYCLE NO.	CYCLE TIME (efps)	CUMULATIVE TIME (efps)	CYCLE AVERAGE FLUX (n/cm2-sec)	CUMULATIVE FLUENCE (n/cm2)
1P	1.87E+07	1.87E+07	9.80E+09	1.83E+17
1C	6.45E+06	2.52E+07	8.23E+09	2.36E+17
2P	1.76E+07	4.28E+07	9.43E+09	4.02E+17
2C	6.04E+06	4.88E+07	8.28E+09	4.52E+17
3P	9.90E+06	5.87E+07	1.15E+10	5.66E+17
3C	9.15E+06	6.78E+07	1.03E+10	6.60E+17
4P	1.70E+07	8.48E+07	1.11E+10	8.49E+17
4C	9.03E+06	9.39E+07	9.83E+10	9.38E+17
5P	2.19E+07	1.16E+08	1.28E+10	1.22E+18
5C	4.90E+06	1.21E+08	1.20E+10	1.28E+18
6P	2.82E+07	1.49E+08	1.11E+10	1.59E+18
6C	9.26E+06	1.58E+08	1.02E+10	1.68E+18
7P	2.70E+07	1.85E+08	1.23E+10	2.01E+18
7C	8.78E+06	1.94E+08	1.12E+10	2.11E+18
8P	2.43E+07	2.18E+08	1.22E+10	2.41E+18
8C	5.59E+06	2.24E+08	1.13E+10	2.47E+18
9P	2.97E+07	2.54E+08	1.14E+10	2.81E+18
9C	6.24E+06	2.60E+08	1.05E+10	2.88E+18
10P	2.94E+07	2.8[illegible]E+08	1.51E+10	3.32E+18
10C	1.05E+07	3.00E+08	1.37E+10	3.46E+18
11P	2.92E+07	3.29E+08	1.48E+10	3.89E+18
11C	4.67E+06	3.34E+08	1.38E+10	3.96E+18
12P	3.68E+07	3.70E+08	1.40E+10	4.47E+18
12C	1.83E+06	3.72E+08	1.33E+10	4.50E+18
13P	3.20E+07	4.0[illegible]E+08	1.35E+10	4.93E+18
13C	1.01E+06	4.[illegible]5E+08	1.33E+10	4.95E+18
14P	3.57E+07	4 41E+08	1.31E+10	5.41E+18
14C	5.66E+06	4.47E+08	1.16E+10	5.48E+18
15P	3.00E+07	4.77E+08	1.36E+10	5.89E+18
15C	3.92E+06	4.80E+08	1.25E+10	5.93E+18
16P	3.51E+07	5.16E+08	1.33E+10	6.40E+18
16C	1.43E+06	5.17E+08	1.28E+10	6.42E+18
17P	3.30E+07	5.50E+08	1.33E+10	6.86E+18
17C	5.47E+06	5.55E+08	1.20E+10	6.92E+18
18P	3.63E+07	5.92E+08	1.31E+10	7.40E+18
18C	4.37E+06	5.96E+08	1.21E+10	7.45E+18
19P	3.24E+07	6.29E+08	1.35E+10	7.89E+18
19C	6.36E+06	6.35E+08	1.20E+10	7.97E+18
20P	3.76E+07	6.72E+08	1.33E+10	8.47E+18
20C	4.44E+06	6.77E+08	1.22E+10	8.52E+18

TABLE 1-8

AZIMUTHAL DISTRIBUTION OF MAXIMUM FAST NEUTRON (E > 1.0 MeV)
FLUENCE AT THE PRESSURE VESSEL INNER RADIUS
(END OF CYCLE 20 - 21.45 EFPY)

THETA (Deg)	FLUENCE (n/cm2)	THETA (Deg)	FLUENCE (n/cm2)
0.50	1.95E+19	23.50	1.76E+19
1.50	1.96E+19	24.50	1.70E+19
2.50	1.99E+19	25.50	1.64E+19
3.43	2.01E+19	26.20	1.60E+19
3.93	2.02E+19	26.60	1.58E+19
4.50	2.04E+19	26.90	1.56E+19
5.50	2.05E+19	27.50	1.52E+19
6.50	2.06E+19	28.21	1.48E+19
7.50	2.07E+19	28.62	1.45E+19
8.50	2.09E+19	29.05	1.42E+19
9.14	2.11E+19	29.47	1.39E+19
9.64	2.11E+19	29.84	1.37E+19
10.50	2.13E+19	30.50	1.33E+19
11.50	2.13E+19	31.50	1.28E+19
12.50	2.14E+19	32.50	1.22E+19
13.50	2.14E+19	33.50	1.17E+19
14.50	2.13E+19	34.50	1.12E+19
15.52	2.10E+19	35.50	1.07E+19
16.19	2.08E+19	36.35	1.04E+19
16.50	2.08E+19	36.90	1.02E+19
16.82	2.08E+19	37.55	9.95E+18
17.50	2.08E+19	38.50	9.69E+18
18.50	2.04E+19	39.50	9.36E+18
19.50	1.99E+19	40.50	9.10E+18
20.50	1.94E+19	41.50	8.90E+18
21.30	1.89E+19	42.50	8.70E+18
21.80	1.86E+19	43.50	8.57E+18
22.50	1.82E+19	44.50	8.51E+18

FIGURE 1-6

AZIMUTHAL DISTRIBUTION OF MAXIMUM FAST NEUTRON (E > 1.0 MeV)
FLUENCE AT THE PRESSURE VESSEL INNER RADIUS
(END OF CYCLE 20 - 21.45 EFPY)

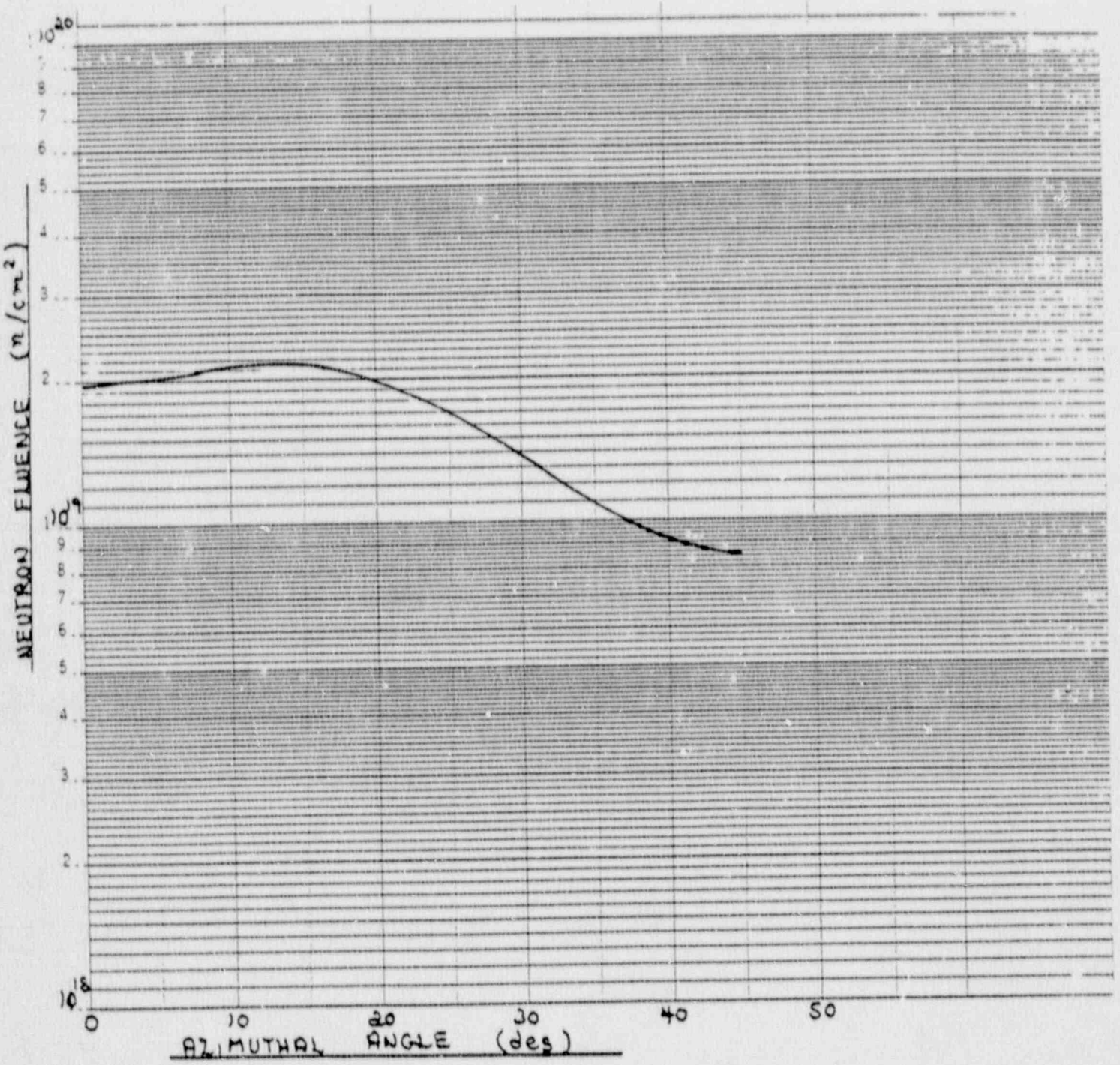

TABLE 1-9

FAST NEUTRON FLUENCE (E > 1.0 MeV) AS A FUNCTION OF RADIAL POSITION WITHIN THE YANKEE ROWE PRESSURE VESSEL (END OF CYCLE 20 - 21.45 EFPY)

RADIUS (cm)	NEUTRON FLUENCE (n/cm2) MAXIMUM	MINIMUM
139.97	2.14E+19	8.51E+18
140.14	2.12E+19	8.44E+18
140.60	2.03E+19	8.11E+18
141.34	1.88E+19	7.59E+18
142.22	1.70E+19	6.86E+18
143.10	1.51E+19	6.15E+18
143.99	1.34E+19	5.50E+18
144.87	1.19E+19	4.88E+18
145.75	1.05E+19	4.33E+18
146.63	9.21E+18	3.84E+18
147.51	8.08E+18	3.40E+18
148.39	7.16E+18	3.00E+18
149.27	6.26E+18	2.65E+18
150.15	5.49E+18	2.34E+18
151.04	4.81E+18	2.06E+18
151.92	4.21E+18	1.81E+18
152.80	3.68E+18	1.59E+18
153.68	3.21E+18	1.39E+18
154.56	2.80E+18	1.22E+18
155.44	2.43E+18	1.07E+18
156.32	2.11E+18	9.30E+17
156.76	1.97E+18	8.71E+17

2.0 ADDITIONAL CALCULATIONS

In addition to the the baseline calculations described in Section 1.0, several additional studies were carried out as a part of this evaluation. The first involved the determination of the effect that the extra baffle structure and thermal shield hardware that is present in the 45-90 degree sector of Figure 1-1 would have on the incident flux on the pressure vessel. The second study was to determine the reduction in exposure due to the presence of spacers and the removal of fuel rods in the core quadrant opposite the sector described in the baseline computations. The third study investigated the impact of variations in the inner radius of the pressure vessel on the incident vessel flux. The fourth study was to determine the increase in vessel exposure rates that would occur following complete removal of the thermal shield.

2.1 Calculation of Vessel Exposure Rates in the 45-90 Degree Sector

In Section 1.0, it was noted that the 0-45 degree sector chosen for the baseline transport calculations was a conservative representation of the geometry of the reactor because the amount of steel structure between the core and the pressure vessel was minimized. To assess the impact of the extra baffle structure and thermal shield support hardware that is actually present in the 45-90 degree sector an additional R,Theta DOT calculation was run using the geometry representative of the 45-90 degree sector shown in Figure 1-1.

In performing the DOT run, the 500 F base case was adjusted to accomodate the extra structure in the geometric model. However, all other input (neutron sources, cross-sections, quadrature) remained the same. The results of the 45-90 degree sector calculation are provided in Table 2-1 as a comparison of the calculated flux at the vessel cladding from the two corresponding 1/8 core models. In regard to the data presented in Table 2-1, it should be noted that the order of azimuthal angle runs from 0-45 degrees in the one case and 90-45 degrees in the other. This permits the comparison of data on a one to one basis; i.e. 0.50 degrees in the 0-45 model is equivalent to 89.5 degrees in the 45-90 model.

An examination of Table 2-1 shows that in the 45-90 degree sector incident flux levels at the pressure vessel clad are either equivalent to or somewhat less than corresponding values from the baseline computation. The maximum flux reduction afforded by the presence of the additional structural material is on the order of 5-7%.

2.2 Impact of Core Spacers and Fuel Rod Removal

A schematic of the Yankee Rowe baffle cavity is shown in Figure 2-1. The baseline transport calculations described in Section 1.0 conservatively positioned the core in the upper right quadrant relative to the configuration depicted in Figure 2-1. This positioning placed fuel directly against the baffle plates on all peripheral fuel surfaces. In the opposite quadrant (lower left on Figure 2-1), however, the presence of stainless steel spacers resulted in fuel being displaced from the baffle plates by one row of fuel. During the first 17 cycles of operation fuel bearing rods were in place at the end of each spacer. However, subsequent to cycle 17 these rods were removed creating an entire row of non-fuel bearing area adjacent to the core baffle.

TABLE 3-1

FAST NEUTRON FLUX (E > 1.0 MeV) AT THE PRESSURE VESSEL CLAD
IN THE 0-45 AND 45-90 DEGREE SECTORS
CYCLE 1-16 AVERAGE POWER DISTRIBUTION - 500 F DOWNCOMER

THETA (Deg)	NEUTRON FLUX (n/cm2-sec) 0-45	90-45	THETA (Deg)	NEUTRON FLUX (n/cm2-sec) 0-45	90-45
0.50	2.98E+10	2.80E+10	23.50	2.69E+10	2.68E+10
1.50	3.00E+10	2.82E+10	24.50	2.60E+10	2.59E+10
2.50	3.04E+10	2.86E+10	25.50	2.51E+10	2.50E+10
3.43	3.07E+10	2.90E+10	26.20	2.45E+10	2.43E+10
3.93	3.09E+10	2.93E+10	26.60	2.41E+10	2.38E+10
4.50	3.11E+10	2.95E+10	26.90	2.38E+10	2.34E+10
5.50	3.13E+10	2.99E+10	27.50	2.32E+10	2.27E+10
6.50	3.15E+10	3.01E+10	28.21	2.26E+10	2.20E+10
7.50	3.17E+10	3.04E+10	28.62	2.22E+10	2.15E+10
8.50	3.19E+10	3.05E+10	29.05	2.17E+10	2.10E+10
9.14	3.22E+10	3.06E+10	29.47	2.13E+10	2.05E+10
9.64	3.23E+10	3.07E+10	29.84	2.09E+10	2.01E+10
10.50	3.25E+10	3.06E+10	30.50	2.03E+10	1.94E+10
11.50	3.26E+10	3.04E+10	31.50	1.95E+10	1.86E+10
12.50	3.27E+10	3.04E+10	32.50	1.86E+10	1.79E+10
13.50	3.27E+10	3.04E+10	33.50	1.78E+10	1.72E+10
14.50	3.26E+10	3.04E+10	34.50	1.71E+10	1.67E+10
15.52	3.21E+10	3.03E+10	35.50	1.64E+10	1.61E+10
16.19	3.18E+10	3.03E+10	36.35	1.59E+10	1.57E+10
16.50	3.18E+10	3.04E+10	36.90	1.56E+10	1.54E+10
16.82	3.18E+10	3.01E+10	37.55	1.52E+10	1.51E+10
17.50	3.18E+10	2.96E+10	38.50	1.48E+10	1.47E+10
18.50	3.12E+10	2.90E+10	39.50	1.43E+10	1.43E+10
19.50	3.04E+10	2.85E+10	40.50	1.39E+10	1.39E+10
20.50	2.96E+10	2.81E+10	41.50	1.36E+10	1.36E+10
21.30	2.89E+10	2.76E+10	42.50	1.33E+10	1.33E+10
21.80	2.84E+10	2.68E+10	43.50	1.31E+10	1.31E+10
22.50	2.78E+10	2.59E+10	44.50	1.30E+10	1.30E+10

In order to estimate the impact of this core displacement adjoint evaluations at the 44.5 degree azimuth were performed with the neutron sources in these peripheral rods set to zero. For cycles 1-17 the sources in the spacer locations were removed; while, for cycles 18-20 the rods adjacent to the ends of the spacers were also deleted from the calculation.

The results of this adjoint evaluation are summarized in Table 2-2. An examination of the data provided in Table 2-2 and the corresponding information from Table 1-7 shows the following comparison.

FLUENCE WITHOUT SPACERS	8.52E+18
FLUENCE WITH SPACERS	7.88E+18

Thus, to a first approximation the 44.5 degree vessel exposure in the octants containing spacers and deleted fuel rods would be lower than the baseline exposure projections by a factor of 0.925.

2.3 Parameter Study of Vessel Inner Radius

The geometric model used in these fluence evaluations made use of as-built dimensions for the inner radius of the vessel cladding. The nominal radius was established as 139.69 cm. by averaging several measured values provided by Yankee Atomic. The span of these measured radii ranged from a minimum of 139.38 cm. to a maximum of 140.06 cm. Thus, the measurements varied from nominal by from -0.31 to +0.37 cm.

To assess the uncertainty associated with these radial variations a series of one-dimensional ANISN runs was performed using the model described in Section 1.0. The zirconium core calculation was taken as the base case and two additional runs were carried out with the minimum and maximum radii. The following data extracted from the cladding location of each computation demonstrate the impact of vessel radius on the incident exposure rate.

	Relative Flux	Min or Max Nominal
Vessel IR = 139.38 cm	2.237E-07	1.051
Vessel IR = 139.69 cm	2.129E-07	1.000
Vessel IR = 140.05 cm	2.008E-07	0.943

As can be seen from the above tabulation, the uncertainty associated with vessel radius is on the order of +/- 5-6 %.

FIGURE 2-1

SCHEMATIC OF YANKEE ROWE BAFFLE CAVITY

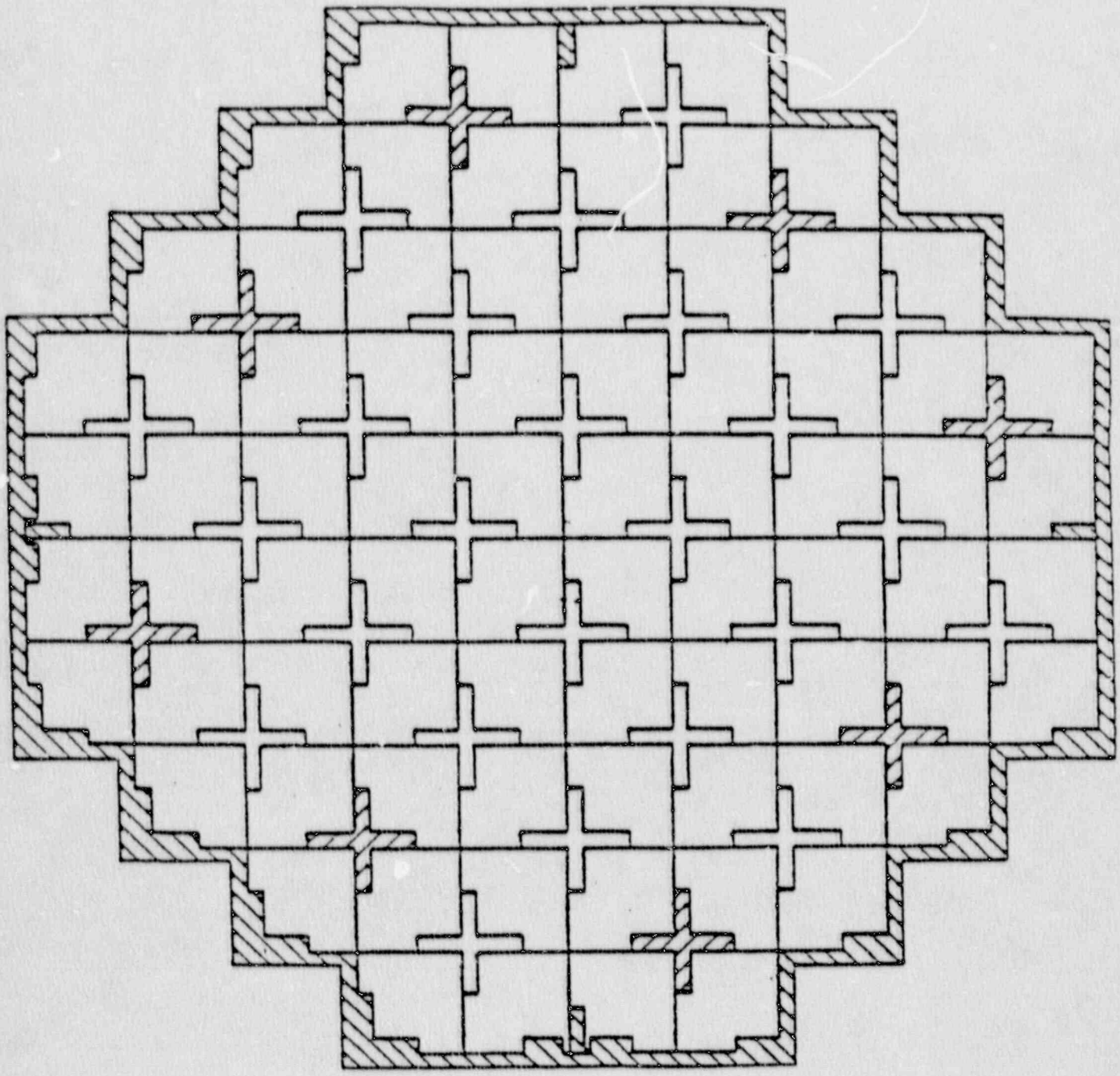

TABLE 2-2

SUMMARY OF FAST NEUTRON (E > 1.0 MeV) FLUX AND FLUENCE AT THE 44.5 DEGREE AZIMUTHAL LOCATION WITH PERIPHERAL FUEL RODS REMOVED

CYCLE NO.	CYCLE TIME (efps)	CUMULATIVE TIME (efps)	CYCLE AVERAGE FLUX (n/cm2-sec)	CUMULATIVE FLUENCE (n/cm2)
1P	1.87E+07	1.87E+07	9.13E+09	1.71E+17
1C	6.45E+06	2.52E+07	7.67E+09	2.20E+17
2P	1.76E+07	4.28E+07	8.79E+09	3.75E+17
2C	6.04E+06	4.88E+07	7.73E+09	4.22E+17
3P	9.90E+06	5.87E+07	1.07E+10	5.27E+17
3C	9.15E+06	6.78E+07	9.55E+09	6.15E+17
4P	1.70E+07	8.48E+07	1.03E+10	7.90E+17
4C	9.03E+06	9.39E+07	9.15E+10	8.73E+17
5P	2.19E+07	1.16E+08	1.19E+10	1.13E+18
5C	4.90E+06	1.21E+08	1.11E+10	1.19E+18
6P	2.82E+07	1.49E+08	1.03E+10	1.48E+18
6C	9.26E+06	1.58E+08	9.45E+09	1.56E+18
7P	2.70E+07	1.85E+08	1.14E+10	1.87E+18
7C	8.78E+06	1.94E+08	1.04E+10	1.96E+18
8P	2.43E+07	2.18E+08	1.13E+10	2.24E+18
8C	5.59E+06	2.24E+08	1.05E+10	2.30E+18
9P	2.97E+07	2.54E+08	1.07E+10	2.61E+18
9C	6.24E+06	2.60E+08	9.80E+09	2.68E+18
10P	2.94E+07	2.89E+08	1.09E+10	3.09E+18
10C	1.05E+07	3.00E+08	1.27E+10	3.22E+18
11P	2.92E+07	3.29E+08	1.37E+10	3.62E+18
11C	4.67E+06	3.34E+08	1.28E+10	3.68E+18
12P	3.68E+07	3.70E+08	1.30E+10	4.16E+18
12C	1.83E+06	3.72E+08	1.24E+10	4.18E+18
13P	3.20E+07	4.04E+08	1.26E+10	4.58E+18
13C	1.01E+06	4.05E+08	1.23E+10	4.59E+18
14P	3.57E+07	4.41E+08	1.22E+10	5.03E+18
14C	5.66E+06	4.47E+08	1.08E+10	5.09E+18
15P	3.00E+07	4.77E+08	1.26E+10	5.47E+18
15C	3.92E+06	4.80E+08	1.16E+10	5.51E+18
16P	3.51E+07	5.16E+08	1.23E+10	5.95E+18
16C	1.43E+06	5.17E+08	1.19E+10	5.96E+18
17P	3.30E+07	5.50E+08	1.24E+10	6.37E+18
17C	5.47E+06	5.55E+08	1.11E+10	6.43E+18
18P	3.68E+07	5.92E+08	1.18E+10	6.86E+18
18C	4.37E+06	5.96E+08	1.09E+10	6.91E+18
19P	3.24E+07	6.29E+08	1.22E+10	7.31E+18
19C	6.36E+06	6.35E+08	1.09E+10	7.37E+18
20P	3.76E+07	6.72E+08	1.20E+10	7.83E+18
20C	4.44E+06	6.77E+08	1.10E+10	7.88E+18

2.4 Thermal Shield Removal

The impact of thermal shield removal on the exposure of the reactor pressure vessel was determined by rerunning the baseline 500 F forward DOT calculation with the thermal shield (zone 5 or Figure 1-2) replaced with downcomer water at 500 F. The results of the evaluation are provided on Table 2-3.

From Table 2-3 it is noted that, depending on azimuthal angle, the removal of the thermal shield would cause an increase in the fast neutron exposure rate at the pressure vessel inner radius by a factor of from 1.39 to 1.50. This variation with angle is caused by the varying steel/water ratio, but in this case does not exhibit a large swing from 0 - 45 degrees.

TABLE 2-3

FAST NEUTRON FLUX (E > 1.0 MeV) AT THE PRESSURE VESSEL CLAD
WITH AND WITHOUT THE THERMAL SHIELD IN PLACE
CYCLE 1-20 AVERAGE POWER DISTRIBUTION - 500 F DOWNCOMER

	NEUTRON FLUX (n/cm2-sec)				NEUTRON FLUX (n/cm2-sec)		
THETA (Deg)	WITH THERMAL SHIELD	WITHOUT THERMAL SHIELD	RATIO	THETA (Deg)	WITH THERMAL SHIELD	WITHOUT THERMAL SHIELD	RATIO
0.50	2.98E+10	4.15E+10	1.39	23.50	2.69E+10	3.86E+10	1.43
1.50	3.00E+10	4.20E+10	1.40	24.50	2.60E+10	3.75E+10	1.44
2.50	3.04E+10	4.27E+10	1.40	25.50	2.51E+10	3.63E+10	1.45
3.43	3.07E+10	4.33E+10	1.41	26.20	2.45E+10	3.55E+10	1.45
3.93	3.09E+10	4.35E+10	1.41	26.60	2.41E+10	3.50E+10	1.45
4.50	3.11E+10	4.38E+10	1.41	26.90	2.38E+10	3.46E+10	1.45
5.50	3.13E+10	4.41E+10	1.41	27.50	2.32E+10	3.37E+10	1.45
6.50	3.15E+10	4.42E+10	1.40	28.21	2.26E+10	3.30E+10	1.46
7.50	3.17E+10	4.45E+10	1.40	28.62	2.22E+10	3.24E+10	1.46
8.50	3.19E+10	4.50E+10	1.41	29.05	2.17E+10	3.18E+10	1.47
9.14	3.22E+10	4.55E+10	1.41	29.47	2.13E+10	3.13E+10	1.47
9.64	3.23E+10	4.58E+10	1.42	29.84	2.09E+10	3.08E+10	1.47
10.50	3.25E+10	4.61E+10	1.42	30.50	2.03E+10	2.99E+10	1.47
11.50	3.26E+10	4.60E+10	1.41	31.50	1.95E+10	2.87E+10	1.47
12.50	3.27E+10	4.57E+10	1.40	32.50	1.86E+10	2.75E+10	1.48
13.50	3.27E+10	4.56E+10	1.39	33.50	1.78E+10	2.63E+10	1.48
14.50	3.26E+10	4.55E+10	1.40	34.50	1.71E+10	2.53E+10	1.48
15.52	3.21E+10	4.55E+10	1.42	35.50	1.64E+10	2.43E+10	1.48
16.19	3.18E+10	4.49E+10	1.41	36.35	1.59E+10	2.36E+10	1.48
16.50	3.18E+10	4.48E+10	1.41	36.90	1.56E+10	2.32E+10	1.49
16.82	3.18E+10	4.46E+10	1.40	37.55	1.52E+10	2.27E+10	1.49
17.50	3.18E+10	4.44E+10	1.40	38.50	1.48E+10	2.21E+10	1.49
18.50	3.12E+10	4.35E+10	1.39	39.50	1.43E+10	2.15E+10	1.50
19.50	3.04E+10	4.24E+10	1.39	40.50	1.39E+10	2.10E+10	1.51
20.50	2.96E+10	4.14E+10	1.40	41.50	1.36E+10	2.05E+10	1.51
21.30	2.89E+10	4.06E+10	1.40	42.50	1.33E+10	2.00E+10	1.50
21.80	2.84E+10	4.01E+10	1.41	43.50	1.31E+10	1.97E+10	1.50
22.50	2.78E+10	3.95E+10	1.42	44.50	1.30E+10	1.95E+10	1.50

3.0 - COMPARISON OF EXPOSURE CALCULATIONS WITH MEASUREMENTS

Surveillance Capsule Measurements

Over the course of the operating lifetime of power reactors, surveillance capsules are periodically withdrawn to provide materials data as well as neutron dosimetry applicable to the specific reactor. These dosimetry results afford the opportunity for power reactor benchmarking that, in turn, permits an assessment of the accuracy of the analytical techniques used to calculate vessel exposures. The following is a summary of comparisons of plant specific calculations with capsule measurements for a variety of Westinghouse reactors.

	Neutron Flux (n/cm2-sec)		
PLANT/CAPSULE	CALCULATED	MEASURED	C/M
A1	9.25E+10	1.01E+11	0.916
B1	1.08E+11	1.34E+11	0.806
C1	9.25E+10	1.06E+11	0.873
D1	9.58E+10	1.01E+11	0.949
E1	9.44E+10	1.05E+11	0.899
F1	1.07E+11	1.24E+11	0.863
G1	9.23E+10	9.47E+10	0.975
H1	9.51E+10	1.09E+11	0.872
I1	9.51E+10	1.09E+11	0.872
J1	9.32E+10	1.30E+11	0.717
J2	8.94E+10	1.01E+11	0.885
K1	8.33E+10	1.04E+11	0.801
K2	9.21E+10	1.10E+11	0.837
L1	9.52E+10	1.16E+11	0.821
L2	8.34E+10	9.05E+10	0.922
M1	1.10E+11	1.43E+11	0.769
M2	6.64E+10	8.56E+10	0.776
M3	1.10E+11	1.46E+11	0.753
N1	1.31E+11	1.61E+11	0.814
N2	1.19E+11	1.42E+11	0.838
N3	7.66E+10	8.27E+10	0.926
O1	6.15E+10	6.92E+10	0.889
O2	6.77E+10	7.30E+10	0.927
O3	5.94E+10	6.28E+10	0.946
P1	5.64E+10	6.47E+10	0.872
P2	5.96E+10	6.84E+10	0.871
P3	5.41E+10	4.99E+10	1.084
Q1	6.45E+10	7.47E+10	0.863
Q2	7.04E+10	8.43E+10	0.835
Q3	7.26E+10	7.12E+10	1.020
Q4	6.33E+10	5.78E+10	1.095
AVERAGE C/M RATIO FOR 31 SURVEILLANCE DATA POINTS			0.880
1 SIGMA STANDARD DEVIATION OF THE DATA BASE			0.085

From this surveillance capsule data base, it is seen that at the capsule locations calculated values using the current radiation transport methodology tend to be low relative to measurement by about 12 %.

Reactor Cavity Measurements

Over the course of the last decade many utilities, either because of a need for very accurate fluence evaluations for regulatory concerns or as a mode of data aquisition to establish a life extension data base, have installed neutron dosimetry in the annular space between the outer radius of the reactor vessel and the inner radius of the primary biological shield. Programs have been in place since 1983 and comparisons of calculations with measured data from these programs provide an additional means to benchmark analytical capability against data obtained directly from power reactor facilities. The following is a summary of comparisons of plant specific calculations with cavity dosimetry measurements from a variety of Westinghouse reactors.

Neutron Flux (n/cm2-sec)

PLANT/DATA POINT	CALCULATED	MEASURED	C/M
R1	6.86E+08	8.13E+08	0.844
R2	6.14E+08	6.75E+08	0.910
R3	4.01E+08	3.78E+08	1.061
R4	2.75E+08	2.99E+08	0.920
R5	5.65E+08	6.49E+08	0.871
R6	5.25E+08	6.37E+08	0.824
R7	2.97E+08	3.28E+08	0.905
R8	2.40E+08	3.17E+08	0.757
S1	6.62E+08	8.22E+08	0.805
S2	6.44E+08	6.37E+08	1.011
S3	6.60E+08	6.99E+08	0.944
S4	4.92E+08	5.41E+08	0.909
S5	5.07E+08	6.65E+08	0.762
S6	4.64E+08	5.82E+08	0.797
S7	4.23E+08	4.02E+08	1.052
S8	3.39E+08	3.70E+08	0.916
T1	5.36E+08	5.51E+08	0.973
T2	4.44E+08	4.57E+08	0.972
T3	3.33E+08	3.58E+08	0.930
T4	2.04E+08	2.34E+08	0.872
T5	5.25E+08	6.39E+08	0.822
T6	4.44E+08	5.10E+08	0.871
T7	3.83E+08	4.34E+08	0.882
T8	2.56E+08	2.79E+08	0.918

Neutron Flux (n/cm2-sec)

PLANT/DATA POINT	CALCULATED	MEASURED	C/M
U1	4.76E+08	5.53E+08	0.861
U2	4.16E+08	5.12E+08	0.813
U3	3.70E+08	4.39E+08	0.843
U4	2.40E+08	2.94E+08	0.816
V1	1.73E+09	1.87E+09	0.925
V2	1.45E+09	1.69E+09	0.858
V3	1.12E+09	1.23E+09	0.911
V4	9.28E+08	1.10E+09	0.844
AVERAGE C/M RATIO FOR 32 CAVITY DATA POINTS			0.887
1 SIGMA STANDARD DEVIATION OF THE DATA BASE			0.073

From this cavity dosimetry data base, it is seen that at the cavity sensor locations calculated values using the current radiation transport methodology tend to be low relative to measurement by about 11 %. This observation is fully consistent with the previous comparisons from the surveillance capsule data base.

Maine Yankee Measurements

In addition to the data base comparisons on Westinghouse designed reactors, the current Westinghouse radiation transport methodology was used for an analysis of the Maine Yankee reactor that included a comparison of calculation with dosimetry results from both surveillance capsules and reactor cavity. That analysis with the comparative information is documented reference 6. Pertinent calculation/measurement comparisons from that evaluation are as follows:

Neutron Flux (n/cm2-sec)

LOCATION	CALCULATION	MEASUREMENT	C/M
35 DEG ACC. CAPSULE	3.45E+11	4.81E+11	0.717
263 DEG WALL CAPSULE	3.35E+10	3.89E+10	0.861
263 DEG CAVITY - CYCLE 7	6.37E+08	7.98E+08	0.798
263 DEG CAVITY - CYCLE 8	5.16E+08	6.53E+08	0.790
AVERAGE C/M RATIO FOR 4 DATA POINTS			0.792

The observed C/M ratios are slightly lower than the overall Westinghouse data base averages, but are still within approximately 1 sigma of those averages. Thus, the dosimetry comparisons indicate the same trend towards underprediction as was observed with the prior comparisons.

4.0 REFERENCES

1 - Soltesz, R. G. et. al., "Nuclear Rocket Shielding Methods, Modification, Updating, and Input Data Preparation - Volume 5 - Two-Dimensional Discrete Ordinates Transport Technique", WANL-PR-(LL)-034, August 1970.

2 - Soltesz, R. G. et. al., "Nuclear Rocket Shielding Methods, Modification, Updating, and Input Data Preparation - Volume 4 - One-Dimensional Discrete Ordinates Transport Technique", WANL-PR-(LL)-034, August 1970.

3 - Yankee Atomic Electric Company letter # RP90-163, Kevin J. Morrissey to S. L. Anderson, June 1, 1990.

4 - SAILOR RSIC DATA LIBRARY COLLECTION DLC-76, "Coupled Self-Shielded, 47 Neutron, 20 Gamma-Ray, P3, Cross Section Library for Light Water Reactors.

5 - Yankee Atomic Electric Company letter # RP90-299, Kevin J. Morrissey to S. L. Anderson, October 5, 1990.

6 - Anderson, S. L. and Lippincott, E. P., "Summary of Fast Neutron Exposure Evaluations for the Maine Yankee Reactor Pressure Vessel", WCAP-11035, November 1986.

Attachment B

Results of the PTS Fracture Mechanics Analysis

Table 1

Fluence Distribution for Beltline Materials

Peak Fluence at 21.44 EFPY (1990)= 2.14 e19 n/cm2

		AZIMUTHAL VARIATION									Axial Welds
		0 to 5	5 to 10	10 to 15	15 to 20	20 to 25	25 to 30	30 to 35	35 to 40	40 to 45	40 to 45
Upper Plate											
	10 to 20	0.300	0.314	0.321	0.302	0.268	0.226	0.183	0.149	0.132	0.132
	20 to 30	1.030	1.077	1.102	1.038	0.919	0.775	0.628	0.510	0.453	0.453
	30 to 40	1.625	1.698	1.738	1.637	1.449	1.222	0.990	0.805	0.714	0.714
	40 to 50	1.853	1.936	1.982	1.867	1.653	1.393	1.130	0.917	0.814	0.814
% of Height	50 to 60	1.947	2.034	2.082	1.961	1.737	1.464	1.187	0.964	0.856	0.856
	60 to 70	1.947	2.034	2.082	1.961	1.737	1.464	1.187	0.964	0.856	0.856
	70 to 80	2.001	2.091	2.140	2.016	1.785	1.504	1.220	0.991	0.880	0.880
	80 to 90	1.965	2.053	2.101	1.980	1.753	1.477	1.198	0.973	0.864	0.864
	90 to 100	1.947	2.034	2.082	1.961	1.737	1.464	1.187	0.964	0.856	0.856
Circ Weld		1.781	1.861	1.905	1.794	1.588	1.339	1.086	0.882	0.783	
Lower Plate											35 to 40
	0 to 10	1.781	1.861	1.905	1.794	1.588	1.339	1.086	0.882	0.783	0.882
% of Height	10 to 20	1.401	1.464	1.498	1.411	1.249	1.053	0.854	0.694	0.616	0.694
	20 to 30	0.808	0.845	0.865	0.814	0.721	0.608	0.493	0.400	0.355	0.400
	30 to 40	0.140	0.146	0.150	0.141	0.125	0.105	0.085	0.069	0.062	0.069

Table 2

Mean Delta RTNDT Distribution for Beltline Materials

Peak Fluence at 21.44 EFPY (1990)= 2.14 e19 n/cm2

		AZIMUTHAL VARIATION									Axial Welds
		0 to 5	5 to 10	10 to 15	15 to 20	20 to 25	25 to 30	30 to 35	35 to 40	40 to 45	40 to 45
Upper Plate											
	10 to 20	102	105	106	103	96	87	78	70	66	157
	20 to 30	192	195	197	193	184	170	154	138	129	227
	30 to 40	222	225	226	223	215	204	189	173	164	255
	40 to 50	230	233	234	230	223	213	199	183	174	263
% of Height	50 to 60	233	236	237	234	226	216	202	187	178	267
	60 to 70	233	236	237	234	226	216	202	187	178	267
	70 to 80	235	237	239	235	228	217	204	189	180	268
	80 to 90	234	236	238	234	227	216	203	188	179	267
	90 to 100	233	236	237	234	226	216	202	187	178	267
Circ Weld		312	315	316	313	305	295	282	269	261	
Lower Plate											35 to 40
	0 to 10	308	310	312	308	301	290	276	260	251	269
% of Height	10 to 20	293	296	297	293	286	274	258	242	232	253
	20 to 30	254	257	259	254	245	231	216	201	193	219
	30 to 40	148	149	150	148	144	139	134	130	128	129

Note: To determine the reference temperature, an initial temperature of 30F for plates and 10F for welds must be added to these mean reference temperatures.

Table 3

PTS Fracture Mechanics Results

	1990 Peak Fluence (x 1E+19 n/cm2)	Peak Reference Temperature (F)	Conditional Failure Probability
Upper Plate	2.14	269	5.60E-04
Lower Plate	1.9	342	4.00E-06
Circ. Weld	1.9	326	1.30E-04
Upper Axial Weld	0.88	278	5.80E-03
Lower Axial Weld	0.88	279	2.00E-05
			6.51E-03